Paper III

Numerical simulation of elastic vibrations using a velocity-stress formulation

Marcus Berglund

Royal Institute of Technology, NADA
S-100 44, Stockholm Sweden
email: marcus@nada.kth.se

3.1 Elastic wave equation

Consider a Cartesian coordinate system for three space dimensions with coordinates x_1, x_2, x_3 and unit vectors $\bar{e}_1$, $\bar{e}_2$, $\bar{e}_3$. We can express a vector $\bar{v}$ as $\bar{v} = \sum_{k=1}^{3} v_k \bar{e}_k$. By using the so called summation convention: whenever an index appears twice in an expression, the expression is assumed to be summed over the range of the index, we can write the vector $\bar{v}$ as $\bar{v} = v_k \bar{e}_k$. With this convention we can easily express the scalar product between to vectors as $\bar{u} \cdot \bar{v} = u_k v_k$.

In vector notation, Newton's second law is, $\bar{F} = m\bar{a}$, and in index notation, $F_1 = ma_1$, $F_2 = ma_2$, $F_3 = ma_3$. Using another convention: whenever an index appears once in each term of an equation, the equation is assumed to hold for each value in the range of the index. With this convention , we write Newton's second law as $F_k = ma_k$.

The partial derivative with respect to x_i of the scalar field $f(x_1, x_2, x_3)$ can be written by another index notation as

$$\frac{\partial f}{\partial x_i} = f_{,i}.$$

Using the summation convention we can express the divergence of a vector field, $\bar{f}(x_1, x_2, x_3) = f_1(x_1, x_2, x_3)\bar{i}_1 + f_2(x_1, x_2, x_3)\bar{i}_2 + f_3(x_1, x_2, x_3)\bar{i}_3$, as

$$\text{div } \bar{f} = \sum_{k=1}^{3} \frac{\partial f_k}{\partial x_k} = f_{k,k}.$$

We will also use the Kronecker delta,

$$\delta_{ij} = \begin{cases} 1, & \text{if } i = j, \\ 0, & \text{if } i \neq j. \end{cases}$$

Consider the inhomogeneous and isotropic elastic wave equation in tensor notation,

$$\rho u_{i,tt} = \sigma_{ij,j}, \qquad i = 1, 2, 3, \tag{1}$$

where

$$\sigma_{ij} = \lambda(x_1, x_2)\epsilon_{ii}\delta_{ij} + 2\mu(x_1, x_2)\epsilon_{ij},$$
$$\epsilon_{ij} = \frac{1}{2}(u_{i,j} + u_{j,i}),$$

and $\lambda(x_1, x_2),\ \mu(x_1, x_2) \geq \delta > 0$. λ and μ are the so called Lamé parameters and $\rho(x_1, x_2)$ is the density. For a physical motivation of the elastic wave equation, see [BD].

If λ and μ are constants we can easily rewrite elastic wave equation (2 dimensions) as a first order symmetric system. Put $v_r = u_{r,t}$, $r = 1, 2$, $\sigma_1 = u_{1,1} + u_{2,2}$ and $\sigma_2 = u_{1,2} - u_{2,1}$ in (1),

$$\begin{pmatrix} v_1 \\ v_2 \\ \sigma_2 \\ \sigma_1 \end{pmatrix}_t = \underbrace{\begin{pmatrix} 0 & 0 & 0 & \rho^{-1}(\lambda+2\mu) \\ 0 & 0 & -\rho^{-1}\mu & 0 \\ 0 & -1 & 0 & 0 \\ 1 & 0 & 0 & 0 \end{pmatrix}}_{=A_1} \begin{pmatrix} v_1 \\ v_2 \\ \sigma_2 \\ \sigma_1 \end{pmatrix}_{x_1} + \underbrace{\begin{pmatrix} 0 & 0 & \rho^{-1}\mu & \\ 0 & 0 & 0 & \rho^{-1}(\lambda+2\mu) \\ 1 & 0 & 0 & 0 \\ 0 & 1 & 0 & 0 \end{pmatrix}}_{=A_2} \begin{pmatrix} v_1 \\ v_2 \\ \sigma_2 \\ \sigma_1 \end{pmatrix}_{x_2}. \tag{2}$$

Then set

$$\bar{u} = \begin{pmatrix} 1 & 0 & 0 & 0 \\ 0 & 1 & 0 & 0 \\ 0 & 0 & (\mu/\rho)^{1/2} & 0 \\ 0 & 0 & 0 & ((\lambda+2\mu)/\rho)^{1/2} \end{pmatrix} \begin{pmatrix} v_1 \\ v_2 \\ \sigma_2 \\ \sigma_1 \end{pmatrix}$$

and plug this in (2) to obtain,

$$\bar{u}_t = \tilde{A}_1\bar{u}_{x_1} + \tilde{A}_2\bar{u}_{x_2}, \tag{3}$$

where

$$\tilde{A}_1 = \begin{pmatrix} 0 & 0 & 0 & \kappa_3 \\ 0 & 0 & -\kappa_1 & 0 \\ 0 & -\kappa_1 & 0 & 0 \\ \kappa_3 & 0 & 0 & 0 \end{pmatrix}, \quad \tilde{A}_2 = \begin{pmatrix} 0 & 0 & \kappa_1 & 0 \\ 0 & 0 & 0 & \kappa_3 \\ \kappa_1 & 0 & 0 & 0 \\ 0 & \kappa_3 & 0 & 0 \end{pmatrix},$$

and $\kappa_1 = (\mu/\rho)^{1/2}$, $\kappa_3 = ((\lambda+2\mu)/\rho)^{1/2}$.

The system (3) is symmetric and strictly hyperbolic since the symbol,

$$P(\omega) = A_1\omega_1 + A_2\omega_2, \quad \omega_i \text{ real and } \omega_1^2 + \omega_2^2 = 1,$$

has real and distinct eigenvalues,

$$\kappa_{1,2} = \pm(\mu/\rho)^{1/2}, \quad \kappa_{3,4} = \pm((\lambda+2\mu)/\rho)^{1/2}.$$

Unfortunately this simple formulation can not be used when the Lamé parameters are non-constant, so we will not use this formulation.

Now consider λ, μ as functions of x_1 and x_2. This time we take the velocities and stresses, v_i and σ_{ij}, as variables, and rewrite the elastic wave equation as the first order system [V], [TK],

$$\begin{aligned} \bar{w}_t = & \underbrace{\begin{pmatrix} 0 & \rho^{-1} & 0 & 0 & 0 \\ \lambda+2\mu & 0 & 0 & 0 & 0 \\ \lambda & 0 & 0 & 0 & 0 \\ 0 & 0 & 0 & 0 & \rho^{-1} \\ 0 & 0 & 0 & \mu & 0 \end{pmatrix}}_{=B_1} \bar{w}_{x_1} + \\ & \underbrace{\begin{pmatrix} 0 & 0 & 0 & 0 & \rho^{-1} \\ 0 & 0 & 0 & \lambda & 0 \\ 0 & 0 & 0 & \lambda+2\mu & 0 \\ 0 & 0 & \rho^{-1} & 0 & 0 \\ \mu & 0 & 0 & 0 & 0 \end{pmatrix}}_{=B_2} \bar{w}_{x_2}, \end{aligned} \tag{4}$$

where

$$\bar{w} = (w_1,\ w_2,\ w_3,\ w_4,\ w_5)^T = (v_1,\ \sigma_{11},\ \sigma_{22},\ v_2,\ \sigma_{12})^T.$$

The displacements can be obtained by integrating the velocities, since $u_{r,t} = v_r$. This system is also strictly hyperbolic since the symbol,

$$P(\omega) = B_1\omega_1 + B_2\omega_2, \quad \omega_i \text{ real and } \omega_1^2 + \omega_2^2 = 1,$$

has real and distinct eigenvalues,

$$\kappa_1 = 0, \quad \kappa_{2,3} = \pm(\mu/\rho)^{1/2}, \qquad \kappa_{4,5} = \pm((\lambda+2\mu)/\rho)^{1/2}.$$

When λ and μ only depend on x_2 we can by introducing the variable

$$\bar{w} = (u_{1x_1},\ u_{2,x_1},\ u_{1x_2},\ u_{2,x_2},\ u_{1,t},\ u_{2,t},\ u_1,\ u_2)^T,$$

rewrite (1) as a symmetric first order system [J]. So,

$$\begin{aligned} \begin{pmatrix} A_1 & 0 \\ 0 & A_2 \end{pmatrix} \bar{w}_t = & \begin{pmatrix} 0 & B \\ B^T & 0 \end{pmatrix} \bar{w}_{x_1} + \begin{pmatrix} 0 & C \\ C^T & 0 \end{pmatrix} \bar{w}_{x_2} + \\ & \begin{pmatrix} 0 & 0 \\ D_1 & D_2 \end{pmatrix} \bar{w}, \end{aligned} \tag{5}$$

where

$$A_1 = \begin{pmatrix} \lambda+2\mu & 0 & 0 & \frac{1}{2}(\lambda+\mu) \\ 0 & \mu & \frac{1}{2}(\lambda+\mu) & 0 \\ 0 & \frac{1}{2}(\lambda+\mu) & \mu & 0 \\ \frac{1}{2}(\lambda+\mu) & 0 & 0 & \lambda+2\mu \end{pmatrix},$$

$$A_2 = \begin{pmatrix} \rho & 0 & 0 & 0 \\ 0 & \rho & 0 & 0 \\ 0 & 0 & 1 & 0 \\ 0 & 0 & 0 & 1 \end{pmatrix},$$

$$B = \begin{pmatrix} \lambda+2\mu & 0 & 0 & 0 \\ 0 & \mu & 0 & 0 \\ 0 & \frac{1}{2}(\lambda+\mu) & 0 & 0 \\ \frac{1}{2}(\lambda+\mu) & 0 & 0 & 0 \end{pmatrix},$$

$$C = \begin{pmatrix} 0 & \frac{1}{2}(\lambda+\mu) & 0 & 0 \\ \frac{1}{2}(\lambda+\mu) & 0 & 0 & 0 \\ \mu & 0 & 0 & 0 \\ 0 & \lambda+2\mu & 0 & 0 \end{pmatrix},$$

$$D_1 = \begin{pmatrix} 0 & \mu_{x_2} & \mu_{x_2} & 0 \\ 0 & 0 & 0 & (\lambda+2\mu)_{x_2} \\ 0 & 0 & 0 & 0 \\ 0 & 0 & 0 & 0 \end{pmatrix},$$

$$D_2 = \begin{pmatrix} 0 & 0 & 0 & 0 \\ 0 & 0 & 0 & 0 \\ 1 & 0 & 0 & 0 \\ 0 & 1 & 0 & 0 \end{pmatrix}.$$

This formulation will not be used, but shows that it is possible to rewrite (1) as a first order symmetric hyperbolic system.

We can also write (1) as a second order system (λ and μ depend only on x_2),

$$\begin{aligned} \rho \begin{pmatrix} u_1 \\ u_2 \end{pmatrix}_t = & \begin{pmatrix} \lambda+2\mu & 0 \\ 0 & \mu \end{pmatrix} \begin{pmatrix} u_1 \\ u_2 \end{pmatrix}_{x_1x_1} + (\lambda+\mu) \begin{pmatrix} 0 & 1 \\ 1 & 0 \end{pmatrix} \begin{pmatrix} u_1 \\ u_2 \end{pmatrix}_{x_1x_2} + \\ & \begin{pmatrix} \mu & 0 \\ 0 & \lambda+2\mu \end{pmatrix} \begin{pmatrix} u_1 \\ u_2 \end{pmatrix}_{x_2x_2} + \begin{pmatrix} 0 & \partial_{x_2}\mu \\ \partial_{x_2}\lambda & 0 \end{pmatrix} \begin{pmatrix} u_1 \\ u_2 \end{pmatrix}_{x_1} + \\ & \begin{pmatrix} \partial_{x_2}\mu & 0 \\ 0 & \partial_{x_2}(\lambda+2\mu) \end{pmatrix} \begin{pmatrix} u_1 \\ u_2 \end{pmatrix}_{x_2}. \end{aligned}$$

This system is used in section 3.6. We will first concentrate on the first order system (4).

3.2 Initial and boundary conditions

We want to solve (1) on the (physical) domain

$$\Omega_p = \{(x_1, x_2) \in R^2 : -\infty < x_1 < \infty,\ -L_2(x_1) \leq x_2 \leq 0\}, \tag{6}$$

where L_2 is a differentiable function such that $L_2(x_1) \geq \delta > 0$. The initial conditions are,

$$u_1(x_1, x_2, 0) = u_2(x_1, x_2, 0) = \partial_t u_1(x_1, x_2, 0) = \partial_t u_2(x_1, x_2, 0) = 0, \tag{7}$$

The boundary $(x_1, 0)$ is a so-called free-surface (see [BD]) with a load, i.e.

$$\sigma_{12}(x_1, 0) = f_1(x_1, t), \quad \sigma_{22}(x_1, 0) = f_2(x_1, t), \tag{8}$$

where the load f_i are smooth functions with support in $\{(x, t) : 0 < x < L_1,\ t > 0\}$.

At the bottom surface we have zero-displacements, i.e.

$$u_i(x_1, -L(x_1), t) = 0, \qquad i = 1, 2. \tag{9}$$

For computational reasons we want to have a finite computational domain. One way to get a finite computational domain is to bound the physical domain by two extra boundaries. For example put two extra boundaries at $x_1 = 0$ and $x_1 = L_1$, and the new (computational) domain is

$$\Omega_c = \{(x_1, x_2) \in R^2 : 0 < x_1 < L_1,\ -L_2(x_1) < x_2 < 0\}.$$

By using "absorbing boundaries" we introduce absorbing (non-reflecting) boundary conditions. The absorbing boundary conditions should "minimize" reflections from outgoing waves of Ω_c and should not create any ingoing waves and therefore we hope that the solution on Ω_c is a good approximation of the solution on Ω_p. Perfect absorbing boundary conditions exist but they are in general not local in time and space [EM]. Here it is desirable from computational view that the absorbing boundary conditions are local in both time and space. For first order systems a good approximation of absorbing boundary conditions is to set the ingoing characteristic variables equal to zero [EM], [GK]. This is in one space dimension equivalent to the first order paraxial absorbing boundary conditions [EM].

So, for the system (4) we have the initial conditions,

$$\bar{w} = 0, \tag{10}$$

and boundary conditions (11), (12) and (13). The free-surface boundary conditions (8) are

$$w_3(x_1, 0) = f_2, \quad w_5(x_1, 0) = f_1. \tag{11}$$

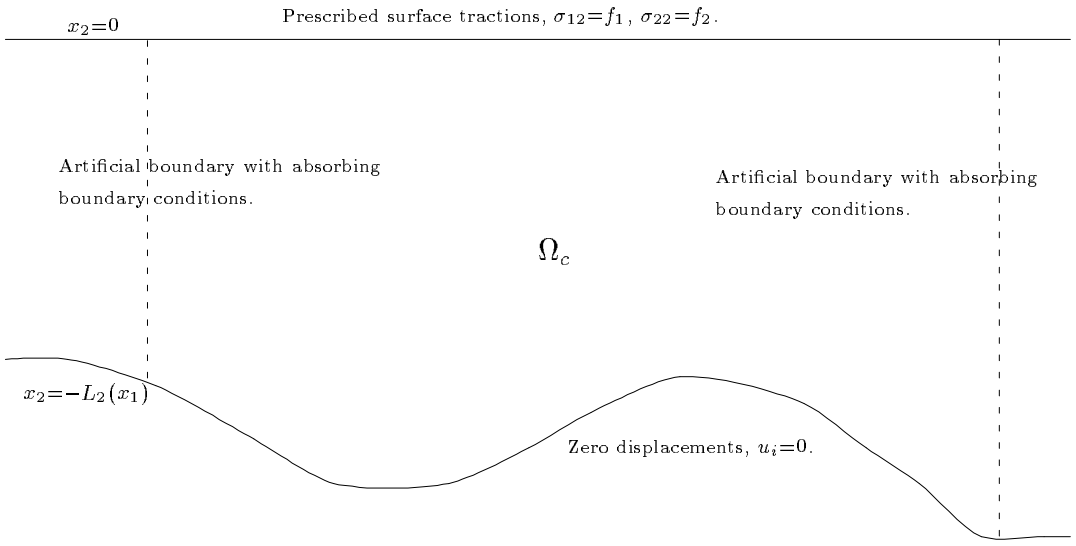

Figure 1: Physical and computational domain and the different boundary conditions.

Note that we can not specify more boundary conditions at $x_2 = 0$ since then the problem will be over-determined because there are only two ingoing characteristic variables [KL]. By taking the time derivative of the zero-displacement conditions (9) we get the zero-velocity conditions,

$$w_1(x_1, -L_2(x_1), t) = w_4(x_1, -L_2(x_1), t) = 0. \tag{12}$$

for (4). The ingoing characteristic variables at $x_1 = 0$ are

$$c_1 = w_4 - (\mu\rho)^{-1/2} w_5, \quad c_2 = -\frac{\lambda\rho^{1/2}}{(\lambda+2\mu)^{1/2}} w_1 + \frac{\lambda}{\lambda+2\mu} w_2,$$

and at $x_1 = L_1$ they are

$$c_1 = w_4 + (\mu\rho)^{-1/2} w_5, \quad c_2 = \frac{\lambda\rho^{1/2}}{(\lambda+2\mu)^{1/2}} w_1 + \frac{\lambda}{\lambda+2\mu} w_2.$$

So, the absorbing boundary conditions are,

$$\begin{aligned}
&w_4(0, x_2, t) - (\mu\rho)^{-1/2} w_5(0, x_2, t) = 0, \\
&-\frac{\lambda\rho^{1/2}}{(\lambda+2\mu)^{1/2}} w_1(0, x_2, t) + \frac{\lambda}{\lambda+2\mu} w_2(0, x_2, t) = 0, \\
&w_4(L_1, x_2, t) + (\mu\rho)^{-1/2} w_5(L_1, x_2, t) = 0, \\
&\frac{\lambda\rho^{1/2}}{(\lambda+2\mu)^{1/2}} w_1(L_1, x_2, t) + \frac{\lambda}{\lambda+2\mu} w_2(L_1, x_2, t) = 0.
\end{aligned} \tag{13}$$

3.3 Lax-Wendroff's method

Consider the initial-boundary value problem (IBVP) (4), (10)-(13) on Ω_c with L_2 constant. On Ω_c we put a uniform $N_1 \times N_2$ grid with grid points indexed by (i,j), $i = 1,2,...,N_1,\ j = 1,2,...,N_2$. Grid point (i,j) has coordinates $(ih_1,(j-N_2)h_2)$, where $h_1 = L_1/(N_1-1)$, $h_2 = L_2/(N_2-1)$, see fig. 2. Grid points with indices (i,j), $i = 2,...,N_1-1, j = 2,...,N_2-1$ are called *interior points* and all other points are called *boundary points*.

Let $\bar{w}^n(i,j)$ be the numerical approximation of the exact solution at grid point (i,j) and at time nk, where k is the time step of the numerical method. The numerical algorithm can be written as,

1. initialize $\bar{w}^0 := 0$.
2. $n := 0$.
3. while $nk < T$ do
   a) calculate $\bar{w}^{n+1}$ at all interior points with Lax-Wendroff's method.
   b) calculate $\bar{w}^{n+1}$ at all boundary points with help of the boundary conditions.
   c) $n := n+1$.

   end while

Note that Lax-Wendroff's method uses the values of $\bar{w}^n$ at all boundary points to calculate $\bar{w}^{n+1}$ at the interior points, see (15).

Lax-Wendroff's method for (4) is based on the Taylor expansion of $\bar{w}(t+k)$ and with help of the equation all time derivatives is changed to space derivatives [RM], [LW2], [LW1],

$$\begin{aligned}\bar{w}(t+k) = \bar{w}(t) + k\bar{w}_t(t) + \frac{k^2}{2}\bar{w}_{tt}(t) + O(k^3) = \bar{w}(t) + k[B_1\bar{w}_{x_1}(t) + \\ B_2\bar{w}_{x_2}(t)] + \frac{k^2}{2}\Big(B_1^2\bar{w}_{x_1x_1}(t) + (B_1B_2 + B_1B_2)\bar{w}_{x_1x_2}(t) + \\ B_2^2\bar{w}_{x_2x_2}(t) + \underbrace{B_2(\frac{\partial}{\partial x_2}B_1)}_{C_1}\bar{w}_{x_1}(t) + \underbrace{B_2(\frac{\partial}{\partial x_2}B_2)}_{C_2}\bar{w}_{x_2}(t)\Big).\end{aligned} \tag{14}$$

Since λ and μ are assumed to be known analytically we only need to discretize the space derivatives of $\bar{w}$ with finite differences, so Lax-Wendroff's method is

$$\begin{aligned}\bar{w}^{n+1}(i,j)) = \bar{w}^n((i,j)) + k[B_1D_{0x_1}\bar{w}^n(i,j) + B_2D_{0x_2}\bar{w}^n(i,j)] + \\ \frac{k^2}{2}\Big(B_1^2D_{+x_1}D_{-x_1}\bar{w}^n(i,j) + (B_1B_2 + B_1B_2)D_{0x_1}D_{0x_2}\bar{w}^n(i,j) + \\ B_2^2D_{+x_2}D_{-x_2}\bar{w}^n(i,j) + C_1D_{0x_1}\bar{w}^n(i,j) + C_2D_{0x_2}\bar{w}^n(i,j)\Big),\end{aligned} \tag{15}$$

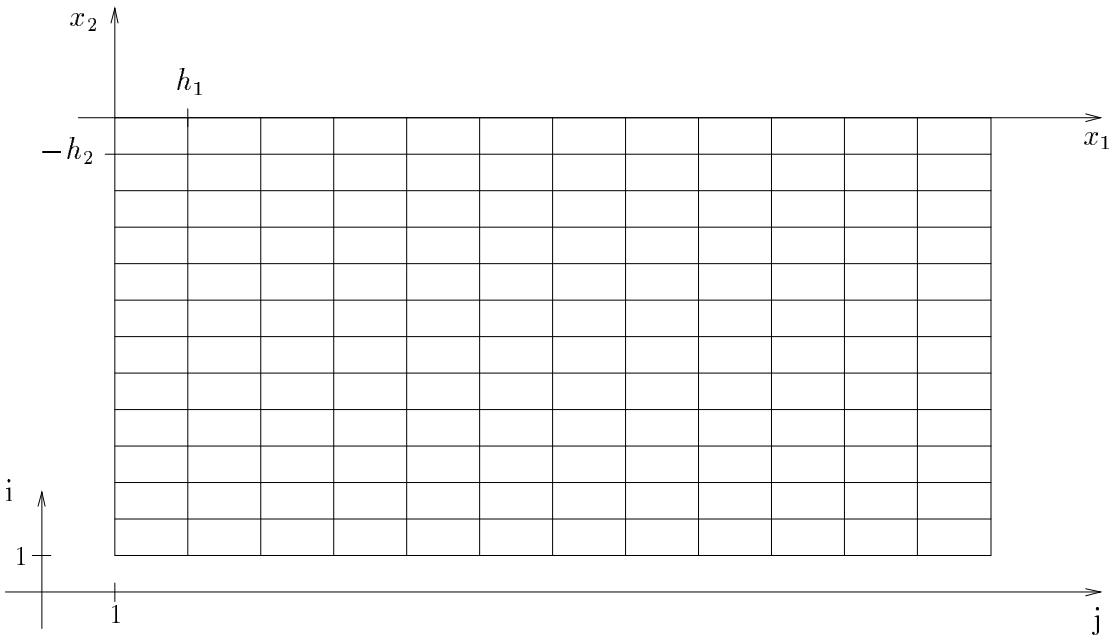

Figure 2: Grid for discretization of elastic wave equation by finite differences.

and B_r, C_r are evaluated at $(x_1, x_2) = ((i-1)h_1, (j-N_2)h_2)$. The difference operators $D_{+\cdot}$, $D_{-\cdot}$ and $D_{0\cdot}$ are defined as usual,

$$\begin{aligned} D_{+x_1}\bar{u}(i,j) &= (\bar{u}(i+1,j) - \bar{u}(i,j))/h_1, \\ D_{-x_1}\bar{u}(i,j) &= (\bar{u}(i,j) - \bar{u}(i-1,j))/h_1, \\ D_{0x_1}\bar{u}(i,j) &= (\bar{u}(i+1,j) - \bar{u}(i-1,j))/2h_1, \\ D_{+x_2}\bar{u}(i,j) &= (\bar{u}(i,j+1) - \bar{u}(i,j))/h_2, \\ &\text{etc.} \end{aligned}$$

This gives step 3a) in the numerical algorithm above.

In step 3b) we begin to update the boundary points with index (i,j), $i = 2, ..., N_1-1$, $j = 1$ with help of the boundary conditions (9), which are discretized as,

$$w_1^n(i,1) = 0, \quad w_4^n(i,1) = 0.$$

Lax-Wendroff's method need also values on w_2, w_3 and w_5 at the boundary points, so we introduce numerical boundary conditions. Here extrapolation of w_2, w_3 and w_5 is used, i.e.

$$D_{+x_2}^q w_2^n(i,1) = D_{+x_2}^q w_3^n(i,2) = D_{+x_2}^q w_5^n(i,2) = 0, \quad q = 1 \text{ or } 2.$$

With $q = 2$ this corresponds to taking one-sided (upwind) differences for w_2, w_3 and w_5 in (15), since if $D^q_{+x_2} w(i,1) = 0$ then

$$D_{0x_2} w(i,2) = \frac{w(i,3) - w(i,1)}{2h_2} = [D^2_{+x_2} w^n(i,1) = 0] = \frac{2(w(i,3) - w(i,2))}{2h_2} = D_{+x_2} w(i,2).$$

In numerical calculations we will only use $q = 2$. Note that the numerical boundary conditions are no real boundary condition which can over-determine the problem [GKS]. In principle the numerical boundary condition is used here to change the discretization of the equation for some of the variables. An alternative is to extrapolate the outgoing characteristic variables, which corresponds to upwind discretization for the characteristic variables.

Next we discretize the absorbing boundary conditions (13) needed to update the boundary points $i = 1, N_1,\ j = 1, ..., N_2 - 1$,

$$w^n_4(1,j) - (\mu\rho)^{-1/2} w^n_5(1,j) = 0, \tag{16a}$$

$$-\frac{\lambda\rho^{1/2}}{(\lambda+2\mu)^{1/2}} w^n_1(1,j) + \frac{\lambda}{\lambda+2\mu} w^n_2(1,j) = 0, \tag{16b}$$

$$w^n_4(N_1,j) + (\mu\rho)^{-1/2} w^n_5(N_1,j) = 0, \tag{16c}$$

$$\frac{\lambda\rho^{1/2}}{(\lambda+2\mu)^{1/2}} w^n_1(N_1,j) + \frac{\lambda}{\lambda+2\mu} w^n_2(N_1,j) = 0. \tag{16d}$$

Here we must extrapolate the outgoing characteristic variables to get the necessary numerical boundary conditions. The numerical boundary conditions are,

$$D^q_{+x_1}(-\lambda w^n_2(1,j) + (\lambda+2\mu) w^n_3(1,j)) = 0, \tag{17a}$$

$$D^q_{+x_1}(w^n_4(1,j) + (\mu\rho)^{-1/2} w^n_5(1,j)) = 0, \tag{17b}$$

$$D^q_{+x_1}(\frac{\lambda\rho^{1/2}}{(\lambda+2\mu)^{1/2}} w^n_1(1,j) + \frac{\lambda}{\lambda+2\mu} w^n_2(1,j)) = 0, \tag{17c}$$

$$D^q_{-x_1}(-\lambda w^n_2(N_1,j) + (\lambda+2\mu) w^n_3(N_1,j)) = 0, \tag{17d}$$

$$D^q_{-x_1}(w^n_4(N_1,j) - (\mu\rho)^{-1/2} w^n_5(N_1,j)) = 0, \tag{17e}$$

$$D^q_{-x_1}(-\frac{\lambda\rho^{1/2}}{(\lambda+2\mu)^{1/2}} w^n_1(N_1,j) + \frac{\lambda}{\lambda+2\mu} w^n_2(N_1,j)) = 0, \tag{17f}$$

where $q = 2$, but $q = 1$ can also be used. It is easily seen that one has 5 linear independent equations per boundary point and 5 unknowns $w^n_r(\cdot,j),\ r = 1, ..., 5$ per boundary point, so $w^n_r(\cdot,j)$ are uniquely determined at every boundary point in question.

Then boundary conditions (11) is used to update the boundary points $i = 2, ..., N_1 - 1,\ j = N_2$,

$$w_3^n(i, N_2) = f_2((i-1)h_1, nk), \quad w_5^n(i, N_2) = f_1((i-1)h_1, nk).$$

The extra numerical boundary conditions are,

$$D_{x_2}^q w_1^n(i, N_2) = D_{-x_2}^q w_2^n(i, N_2) = D_{-x_2}^q w_4^n(i, N_2) = 0$$

where $q = 2$ (or $q = 1$).

Now only two boundary points are left, $i = 1, N_1,\ j = N_2$. It is rather sensitive how the values of w_r are updated. If it is done "wrong" we will get two fast growing spikes in the corners. The values of $w_r^n,\ r = 1, ..., 5$ at the boundary points $i = 2, N_1 - 1,\ j = N_2$ are extrapolated to the corner points $i = 1, N_1,\ j = N_2$, i.e.

$$D_{+x_1} w_r^n(i, N_2) = 0, \quad r = 1, ..., 5,\ i = 1, N_1 - 1.$$

This completes step 3b) and the whole numerical algorithm can be continued until $nk > T$.

When we solve inhomogeneous elastic wave equation (4) with the discretization and boundary conditions above, the number of floating point operations per iteration is approximately $220 N_1 N_2$.

3.4 Method of lines

If space is discretized and time is left continuous, we obtain a system of ordinary differential equations, which can be solved by some standard method like classical 4:th order Runge-Kutta. Consider a strongly hyperbolic system,

$$\bar{u}_t = P(\partial/\partial x)\bar{u} = A_1 \bar{u}_{x_1} + A_2 \bar{u}_{x_2},$$

with constant coefficients. Approximate $P(\partial/\partial x)\bar{u}$ by central finite differences,

$$Q\bar{u}(i, j) = A_1 D_{0x_1} \bar{u}(i, j) + D_{0y} \bar{u}(i, j),$$

and obtain a system of ordinary differential equations,

$$\frac{d\bar{u}(i, j)}{dt} = Q\bar{u}(i, j).$$

This system is in general not stable, i.e. the system has solutions which grow like $\exp(at/h)$, $a > 0$ and $h = h_1$ or $h = h_2$. Instead we solve the modified system,

$$\frac{d\bar{u}(i, j)}{dt} = Q\bar{u}(i, j) + \sigma(D_{+x_1} D_{-x_1} + D_{+x_2} D_{-x_2})\bar{u}(i, j),$$

where the last term in the right hand side is the numerical dissipation and $\sigma =$ const. > 0. If we have strictly hyperbolic system with constant coefficients or a symmetric hyperbolic system with variable coefficients then we have that the Cauchy problem for the system of ordinary differential equations is stable for sufficiently large σ [KGO]. If we discretize time with local stable method like classical 4:th order Runge-Kutta then the fully discrete approximation is stable if σ is sufficiently large and $k/h_1,\ k/h_2$ are sufficiently small [K], [KGO]. Probably this is also true for strictly hyperbolic systems with variable coefficients. Therefor we can hope that numerical algorithm below is also stable for an initial-boundary value problem if the boundary conditions are handled correct. If step 3b) is done the same way as for the Lax-Wendroff's method in section 3.3 we see in numerical experiments that the numerical algorithm below is stable.

The numerical algorithm for solving an IBVP with method of lines is,

1. initialize $\bar{u}^0(i,j)$. n:=0.
2. while $kn < T$,
   3. for $r = 1$ to 4 do
      a) $\bar{v}^r(i,j) := \bar{u}^n(i,j) + c(r)\bar{s}^{(r-1)}(i,j)$ for all inner points.
      b) update the boundary points of $\bar{v}^r$ with help of the boundary conditions and $t = (n + c(r))k$.
      c) $\bar{s}^{(r)}(i,j) := Q\bar{v}^r(i,j)$.
   4. $\bar{u}^{n+1}(i,j) := \bar{u}^n(i,j) + k(s^{(1)}(i,j) + 2s^{(2)}(i,j) + 2s^{(3)}(i,j) + s^{(4)}(i,j))/6$.
   5. $n := n + 1$.

where $c(0) = 0,\ c(1) = c(2) = 1/2,\ c(4) = 1$ and k is the time step.

When we solve inhomogeneous elastic wave equation (4) with the method of lines as described above, the number of floating point operations per iteration is approximately $500N_1N_2$.

3.5 More general physical domain

If the function L_2 in (6) is non-constant we can do a coordinate transformation,

$$\begin{aligned} \tilde{x}_1 &= x_1, \\ \tilde{x}_2 &= h(x_1)x_2, \end{aligned}$$

where $h(x_1) = C/L_2(x_1)$, C constant. Ω_p is then transformed onto the domain,

$$\Omega_p' = \{(x_1, x_2) \in R^2 : -\infty < x_1 < \infty,\ -C \le x_2 \le 0\}.$$

and the corresponding computational domain is

$$\Omega_c = \{(x_1, x_2) \in R^2 : 0 < x_1 < L_1,\ -C \le x_2 \le 0\}.$$

By the chain rule,

$$\frac{\partial}{\partial x_1} = \frac{\partial}{\partial \tilde{x}_1} + \frac{h'(\tilde{x}_1)\tilde{x}_2}{h(\tilde{x}_1)}\frac{\partial}{\partial \tilde{x}_2},$$
$$\frac{\partial}{\partial x_2} = h(\tilde{x}_1)\frac{\partial}{\partial \tilde{x}_2}.$$

The inhomogeneous elastic wave equation (4) in the new coordinates is,

$$\bar{w}_t = B_1\bar{w}_{\tilde{x}_1} + \left(\frac{h'\tilde{x}_2}{h}B_1 + hB_2\right)\bar{w}_{\tilde{x}_2} = \tilde{B}_1\bar{w}_{\tilde{x}_1} + \tilde{B}_2\bar{w}_{\tilde{x}_2}, \tag{18}$$

which also is strictly hyperbolic.

The Taylor expansion of $\bar{w}(t+k)$ is

$$\bar{w}(t+k) = \bar{w}(t) + k[\tilde{B}_1\bar{w}_{\tilde{x}_1} + \tilde{B}_2\bar{w}_{\tilde{x}_2}] + \frac{k^2}{2}[\tilde{B}_1^2\bar{w}_{\tilde{x}_1\tilde{x}_1} + \tilde{B}_2\partial_{\tilde{x}_2}(\tilde{B}_2\bar{w}_{\tilde{x}_2}) + \tilde{B}_1\partial_{\tilde{x}_1}(\tilde{B}_2\bar{w}_{\tilde{x}_2}) + \tilde{B}_2\partial_{\tilde{x}_2}(\tilde{B}_1\bar{w}_{\tilde{x}_1})].$$

Note that here we have assumed that B_i only are functions of x_2 and that $\tilde{B}_2$ become a function of both $\tilde{x}_1$ and $\tilde{x}_2$. This increases the complexity of the method a lot for this variant of Lax-Wendroff's method. Per iteration the number of floating point operation is over $400N_1N_2$. Applying the method of lines described in section 3.4 to (18) needs almost no changes and the number floating point operations per iteration is $750N_1N_2$. We conclude that method of lines is more than $9(400/750) \approx 5$ times better than Lax-Wendroff's method since the timestep can in general be chosen a factor 9 larger for method of lines than for Lax-Wendroff's method.

3.6 Second order system

Consider inhomogeneous elastic wave equation (1) where the Lamé parameters, λ, μ, only depend on x_2, then (1) can be written as,

$$\begin{pmatrix} u_1 \\ u_2 \end{pmatrix}_{tt} = \begin{pmatrix} c_p^2 & 0 \\ 0 & c_s^2 \end{pmatrix}\begin{pmatrix} u_1 \\ u_2 \end{pmatrix}_{x_1x_1} + (c_p^2 - c_s^2)\begin{pmatrix} 0 & 1 \\ 1 & 0 \end{pmatrix}\begin{pmatrix} u_1 \\ u_2 \end{pmatrix}_{x_1x_2} + \begin{pmatrix} c_s^2 & 0 \\ 0 & c_p^2 \end{pmatrix}\begin{pmatrix} u_1 \\ u_2 \end{pmatrix}_{x_2x_2} + \begin{pmatrix} 0 & \mu'(x_2)/\rho \\ \lambda'(x_2)/\rho & 0 \end{pmatrix}\begin{pmatrix} u_1 \\ u_2 \end{pmatrix}_{x_1} + \begin{pmatrix} \mu'(x_2)/\rho & 0 \\ 0 & (\lambda'(x_2)+2\mu'(x_2))/\rho \end{pmatrix}\begin{pmatrix} u_1 \\ u_2 \end{pmatrix}_{x_2},$$

where $c_p = ((\lambda(x_2) + 2\mu(x_2))/\rho)^{1/2}$, $c_s = (\mu(x_2)/\rho)^{1/2}$ are the pressure (P-) and shear (S-) wave speed, respectively. Do the same coordinate transformation as in section 3.5 and the system above transforms into

$$\bar{u}_{tt} = A_1\bar{u}_{\tilde{x}_1\tilde{x}_1} + A_2\bar{u}_{\tilde{x}_1\tilde{x}_2} + A_3\bar{u}_{\tilde{x}_2\tilde{x}_2} + A_4\bar{u}_{\tilde{x}_1} + A_5\bar{u}_{\tilde{x}_2} =: L\bar{u}, \tag{19}$$

where $\bar{u} = (u_1,\ u_2)^T$ and

$$A_1 = \begin{pmatrix} c_p^2 & 0 \\ 0 & c_s^2 \end{pmatrix},$$
$$A_2 = \begin{pmatrix} 2x_2h'c_p^2 & h(c_p^2 - c_s^2) \\ h(c_p^2 - c_s^2) & 2x_2h'c_s^2 \end{pmatrix},$$
$$A_3 = \begin{pmatrix} x_2^2h'^2c_p^2 + h^2c_s^2 & x_2hh'(c_p^2 - c_s^2) \\ x_2hh'(c_p^2 - c_s^2) & x_2^2h'^2c_s^2 + h^2c_p^2 \end{pmatrix},$$
$$A_4 = \begin{pmatrix} 0 & \mu'/\rho \\ \lambda'/\rho & 0 \end{pmatrix},$$
$$A_5 = \begin{pmatrix} x_2h''c_p^2 + h\mu'/\rho & h'(c_p^2 - c_s^2) + x_2h'\mu'/\rho \\ h'(c_p^2 - c_s^2) + x_2h'\mu'/\rho & x_2h''c_s^2 + h(\lambda' + 2\mu'/\rho \end{pmatrix}.$$

As in section 3.2 one want to solve (19) on the domain Ω_p with the initial and boundary conditions (7)-(9). The free-surface boundary condition (8) is expressed in u_i as

$$\begin{aligned} &\mu(hu_{1,\tilde{x}_2} + u_{2,\tilde{x}_1}) = f_1, \\ &\lambda u_{1,\tilde{x}_1} + h(\lambda + 2\mu)u_{2,\tilde{x}_2} = f_2, \end{aligned} \tag{20}$$

where we have used that $\tilde{x}_2 = 0$ at the "top" boundary. Assume that f_r have support in $[0, L_1]$ and introduce extra boundaries at $x_1 = 0$ and at $x_1 = L_1$ to get a finite computational domain. The absorbing boundary conditions used are first order paraxial approximation of the elastic wave equation [CE],

$$\begin{aligned} &u_{1,t}(0, \tilde{x}_2, t) = c_p u_{1,\tilde{x}_1}(0, \tilde{x}_2, t), \\ &u_{2,t}(0, \tilde{x}_2, t) = c_s u_{2,\tilde{x}_1}(0, \tilde{x}_2, t), \\ &u_{1,t}(L_1, \tilde{x}_2, t) = -c_p u_{1,\tilde{x}_1}(L_1, \tilde{x}_2, t), \\ &u_{2,t}(L_1, \tilde{x}_2, t) = -c_s u_{2,\tilde{x}_1}(L_1, \tilde{x}_2, t). \end{aligned} \tag{21}$$

Let $\bar{u}^n(i,j)$ be the numerical approximation of the exact solution, at the grid point (i,j) and at time nk, of (19) with data (7)-(9) and (21). The grid used is similar to the grid in section 3.3, but with the difference that the grid point (i,j) have coordinate $((i-1)h_1, (j+1-N_2)h_2)$, where $h_1 = L_1/(N_1 - 1)$ and $h_2 = L_2/(N_2 - 2)$. The numerical algorithm used to calculate $\bar{u}^n$ can be described as,

1. initialize $\bar{u}^0 = 0$.
2. $n := 0$.
3. while $nk < T$ do
   a) calculate $\bar{u}^{n+1}$ at all interior points with the Leapfrog method.
   b) calculate $\bar{u}^{n+1}$ at all boundary points with help of the boundary conditions.

c) $n := n + 1$.

end while

The Leapfrog method for the system (19) is,

$$\frac{\bar{u}^{n+1}(i,j) - 2\bar{u}^n(i,j) - \bar{u}^{n-1}(i,j)}{k^2} = Q\bar{u}^n(i,j), \tag{22}$$

where

$$\begin{aligned} Q\bar{u}(i,j) = {} & A_1 D_{+\tilde{x}_1} D_{-\tilde{x}_1} \bar{u}^n(i,j) + A_2 D_{0\tilde{x}_1} D_{0\tilde{x}_2} \bar{u}^n(i,j) + A_3 D_{+\tilde{x}_2} D_{-\tilde{x}_2} \bar{u}^n(i,j) + \\ & A_4 D_{0\tilde{x}_1} \bar{u}^n(i,j) + A_5 D_{0\tilde{x}_2} \bar{u}^n(i,j). \end{aligned}$$

This difference approximation is in general not stable together with boundary conditions so we add the damping,

$$-\alpha(\bar{u}^n(i,j) - \bar{u}^{n-1}(i,j))/k + \beta(Q\bar{u}^n(i,j) - Q\bar{u}^{n-1}(i,j))/k, \quad \alpha, \beta \geq 0, \tag{23}$$

to the right hand side of (22). We can relate this numerical damping with the common Rayleigh damping [E], [B], where $-\alpha\bar{u}_t + \beta\partial_t(L\bar{u})$ is added to the right hand side of (19). This completes the step 3a) in the numerical algorithm.

In step 3b) we first make use of the zero-displacement boundary condition to set $\bar{u}^{n+1}(i,1) = 0$, $i = 1, ...N_1$. Next the free-surface boundary condition is used to update $\bar{u}^{n+1}(i,N_2)$, $i = 2, ..., N_1 - 1$. The free-surface boundary condition is discretized as

$$\begin{aligned} \mu h D_{0\tilde{x}_2} u_1^{n+1}(i, N_2 - 1) &= -\mu D_{0\tilde{x}_1} u_2^{n+1}(i, N_2 - 1) + f_1(x_i, t_n), \\ h(\lambda + 2\mu) D_{0\tilde{x}_2} u_2^{n+1}(i, N_2 - 1) &= -\lambda D_{0,\tilde{x}_1} u_1^{n+1}(i, N_2 - 1) + f_2(x_i, t_n), \end{aligned}$$

for $i = 3, ..., N_1 - 2$ and as

$$\begin{aligned} \mu h D_{0\tilde{x}_2} u_1^{n+1}(2, N_2 - 1) &= -\mu D_{+\tilde{x}_1} u_2^{n+1}(1, N_2 - 1) + f_1(x_2, t_n), \\ h(\lambda + 2\mu) D_{0\tilde{x}_2} u_2^{n+1}(2, N_2 - 1) &= -\lambda D_{+,\tilde{x}_1} u_1^{n+1}(2, N_2 - 1) + f_2(x_2, t_n), \\ \mu h D_{0\tilde{x}_2} u_1^{n+1}(N_1 - 1, N_2 - 1) &= -\mu D_{-\tilde{x}_1} u_2^{n+1}(N_1 - 1, N_2 - 1) + \\ & \quad f_1(x_{N_1-1}, t_n), \\ h(\lambda + 2\mu) D_{-\tilde{x}_2} u_2^{n+1}(N_1 - 1, N_2 - 1) &= -\lambda D_{0,\tilde{x}_1} u_1^{n+1}(N_1 - 1, N_2 - 1) + \\ & \quad f_2(x_{N_1-1}, t_n), \end{aligned}$$

where $x_i = (i-1)h_1$, $t_n = (n+1)k$. Now it's a simple task to isolate $\bar{u}^{n+1}(i,N_2)$ for $i = 2, ..., N_1 - 1$. Finally $\bar{u}^{n+1}$ is updated at the remaining boundary points by the absorbing boundary conditions (21) which are discretized as,

$$\frac{u_1^{n+1}(1,j) - u_1^n(1,j)}{k} = c_p D_{0\tilde{x}_1} u_1^n(2,j),$$

$$\frac{u_2^{n+1}(1,j) - u_2^n(1,j)}{k} = c_s D_{0\tilde{x}_1} u_2^n(2,j),$$
$$\frac{u_1^{n+1}(N_1,j) - u_1^n(N_1,j)}{k} = c_p D_{0\tilde{x}_1} u_1^n(N_1-1,j),$$
$$\frac{u_2^{n+1}(N_1,j) - u_2^n(N_1,j)}{k} = c_s D_{0\tilde{x}_1} u_2^n(N_1-1,j).$$

This makes step 3b) and the numerical algorithm complete.

The number of floating point operations per iteration is approximately $190 N_1 N_2$.

3.7 Numerical results

We will investigate three different numerical methods, RK, LW and SEC for solving inhomogeneous elastic wave equation. Here RK corresponds to the method of lines described in section 3.4, LW corresponds to the Lax-Wendroff's method described in section 3.3 and SEC is the Leap-frog method applied to the second order system, see section 3.6. Let $u_{r,X}$ denote the numerical approximation from method X of the displacement in direction x_r, where X = RK, LW or SEC. Let $v_{r,X}$ denote the numerical approximation from method X of the velocity $(\partial_t u_r)$ in direction x_r, where X = RK, LW or SEC. When analytical solutions of the displacements and velocities are available they are denoted by $u_{r,\text{exact}}$ and $v_{r,\text{exact}}$, respectively.

The *first test case* is to solve the homogeneous (constant coefficients) elastic wave equation on the domain $\Omega_c \times R^+ = \{(x_1,x_2) \in R^3 : 0 < x_1 < 32,\ -32 < x_2 < 0,\ t > 0\} \times \{t \in R : t > 0\}$ and physical initial and boundary data,

$$\begin{aligned}
&u_1(x_1,x_2,0) = u_2(x_1,x_2,0) = 0 && (x_1,x_2) \in \Omega_c,\\
&u_1(x_1,-32,t) = u_2(x_1,-32,t) = 0, && 0 < x_1 < 32,\ t > 0,\\
&\sigma_{12}(x_1,0,t) = 0,\ \sigma_{22}(x_1,0,t) = \sin^2 5t, && 0 < x_1 < 32,\ t > 0,
\end{aligned}$$

and at the boundaries $x_1 = 0$ and $x_1 = 32$ we use periodic boundary conditions for all variables, i.e. $\bar{w}(0,x_2,t) = \bar{w}(L_1,x_2,t)$, so that the solution will be x_2-independent. This makes it possible to construct an analytic solution, see appendix 3.A. Choose physical relevant values of the density $\rho = 1500$ kg/m^3, Young's modulus $E = 2 \cdot 10^7$ Pa and Poission's constant $\nu = 0.45$ [A]. Thus, the pressure and shear wave speed are $c_p = 224.9$ m/s and $c_s = 67.8$ m/s, respectively [BD]. Take $h_2 = 1$ for both RK, LW and SEC. What N_1 and h_1 are doesn't matter since the physical and numerical solution is independent of x_1. In fig. 3–4 the vertical displacement and the error $u_{2,num} - u_{2,\text{exact}}$ is plotted as a function of time at the point $x_2 = -22$. In fig. 5–6 the vertical velocity and the vertical velocity error $\partial_t u_{2,num} - \partial_t u_{2,\text{exact}}$ are plotted as a function of time at the point $x_2 = -22$. In fig. 7 we compare the solutions of the vertical velocity from RK for different values of the numerical dissipation.

The *second test case* is to solve the inhomogeneous elastic wave equation on the same domain as in the first test case. We take the same physical initial and boundary data. We choose $E = 2 \cdot 10^7 - 1 \cdot 10^6 x_2$ and $\nu = 0.45$. So, the P-speed vary from 225 m/s to 362 m/s and the S-speed vary from 68 m/s to 109 m/s. For this test case we have not constructed an analytical solution, but it's possible by the method of characteristics. Note that this solution also is independent of x_1. Take $h_2 = 1$ for RK, SEC and LW. In fig. 8 the vertical displacement at $(x_1, x_2) = (\cdot, -22)$ from the three different methods is compared. In fig. 9 the vertical velocity at $(x_1, x_2) = (\cdot, -22)$ from RK and LW is compared. In fig. 10 the vertical velocity at $(x_1, x_2) = (\cdot, -22)$ from RK with different numerical dissipation is compared.

In the *third test case* we solve the inhomogeneous elastic wave equation on three different physical domains,

$$\Omega_r = \{(x_1, x_2) : L_r < x_1 < M_r,\ -32 < x_2 < 0\}, \quad r = 1, 2, 3,$$

where $L_1 = 0,\ M_1 = 32,\ -L_2 = M_2 = 300$ and $-L_3 = M_3 = 1200$. Here we let the physical and computational domain coincide. Let $E = 2 \cdot 10^7 - 1 \cdot 10^6 x_2$, $\rho = 1500$ and $\nu = 0.4$. The P- and S-speed vary between 169–273 m/s and 69–111 m/s, respectively. Let the support of the prescribed surface traction at the surface $x_2 = 0$ be contained in a subset of $\{(x_1, 0) : 0 < x_2 < 32\}$. For all domains and numerical methods take $h_1 = h_2 = 1$. For domain Ω_r the initial and boundary conditions are,

$$\begin{aligned}
&u_1(x_1, x_2, 0) = u_2(x_1, x_2, 0) = 0, && (x_1, x_2) \in \Omega_p, \\
&u_1(x_1, -32, t) = u_2(x_1, -32, t) = 0, && -L_r < x_1 < M_r,\ t > 0, \\
&\sigma_{12}(x_1, 0, t) = 0, && -L_r < x_1 < M_r,\ t > 0, \\
&\sigma_{22}(x_1, 0, t) = \begin{cases} \sin(\pi(x_1 - 10)/12) \sin 5t, & 10 < x_1 < 22,\ t > 0, \\ 0, & x_1 \le 10 \text{ or } x_1 \ge 22,\ t > 0. \end{cases}
\end{aligned}$$

To make the numerical scheme stable the Rayleigh damping is used with $\alpha = 0.05,\ \beta = 0.0005$. Note that we don't use LW in the remaining test cases since the computational work for LW is at least a factor five larger than for RK and SEC and the accuracy for LW is no better than for RK and SEC. In fig. 11 the solutions of the vertical displacement from RK and SEC and for the three different domains are plotted as a function of time. In fig. 12 we see for the first order system how reflections from the absorbing boundary effect the solution at $x_2 = 0$. It is clear that the reflections from the artificial boundaries are much larger for the first order system than for the second order system.

In the *fourth test case* we solve the inhomogeneous elastic wave equation on three different wide domains with variable depth,

$$\Omega_r = \{(x_1, x_2) : L_r < x_1 < M_r,\ -L(x_1) < x_2 < 0\},$$

where $L_1 = 0,\ M_1 = 32,\ -L_2 = M_2 = 200,\ -L_3 = M_3 = 1200$ and

$$L(x_1) = \begin{cases} 32/(1 - 0.2\sin(\pi(x_1 - 5)/22)), & 5 < x_1 < 27, \\ 0, & \text{otherwise.} \end{cases}$$

The domain Ω_r is mapped to the computational domain

$$\Omega_r' = \{(x_1', x_2') : L_r < x_1 < M_r, -32 < x_2 < 0\}, \quad K \text{ positive constant,}$$

by the transformation,

$$x_1' := x_1, \qquad x_2' := 32x_2/L(x_1).$$

Let $\nu = 0.4$, $\rho = 1500$ and $E = 2 \cdot 10^7 - 1 \cdot 10^6 x_2$. The P- and S-speed vary between 169–293 m/s and 69–119 m/s, respectively. Take the same surface tractions as in the third test case. For all domains and methods take $h_1 = h_2 = 1$ except in one run where $h_1 = h_2 = 0.5$. In fig. 13 we see the grid, used by RK for the domain Ω_1', mapped back to the physical coordinates (domain). In fig. 14–15 the solutions of the vertical displacement from RK and SEC and the three different domains are plotted as functions of time. In fig. 16 the solutions of the vertical displacement are compared from the two methods RK and SEC, both with the same computational domain.

In all test cases with constant coefficients the maximal timestep agrees well with the theory. For the problems with variable coefficients we define the *local P- and S-speed* by freezing the coefficients and calculate the P- and S-speed from the obtained "local" constant coefficient problem. Let C_p be the (largest local) P-speed for the constant (variable) coefficient problem. Then we can take the timestep $k < 2.8\min(h_1, h_2)/C_p$ for RK, $k < \min(h_1, h_2)/C_p$ for SEC and $k < \min(h_1, h_2)/(\sqrt{11}C_p)$ for LW [LW1], [LW2], .

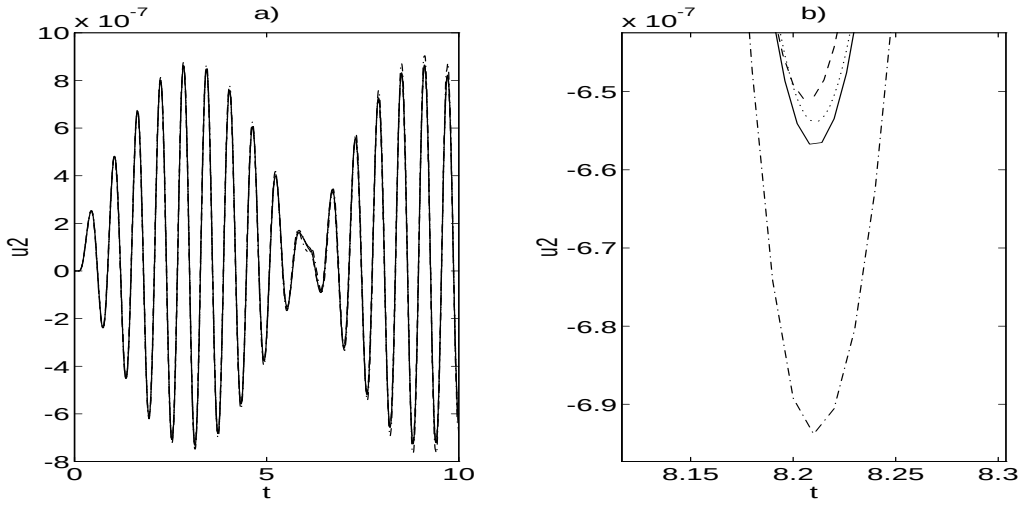

Figure 3: **First test case.** Vertical displacement at $x_2 = -22$ is plotted as a function of time. a) **solid line** – $u_{2,\mathrm{exact}}$, **dashed line** – $u_{2,\mathrm{RK}}$ with $k = 0.005$ and numerical dissipation $\sigma = 5$, **dash dotted line** – $u_{2,\mathrm{LW}}$ with $k = 0.001$, **dotted line** – $u_{2,\mathrm{SEC}}$ with $k = 0.002$. b) zoom of previous plot.

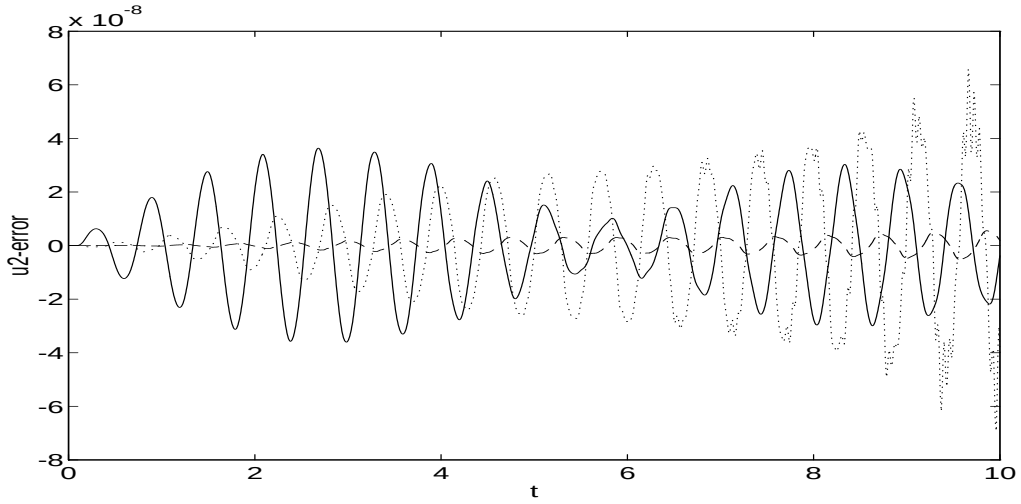

Figure 4: **First test case.** The error of the vertical displacement at $x_2 = -22$ is plotted as a function of time, **solid line** – $u_{2,\mathrm{RK}}$-$u_{2,\mathrm{exact}}$ with $k = 0.005$ and numerical dissipation $\sigma = 5$, **dotted line** – $u_{2,\mathrm{LW}}$-$u_{2,\mathrm{exact}}$ with $k = 0.001$, **dashed line** – $u_{2,\mathrm{SEC}}$-$u_{2,\mathrm{exact}}$ with $k = 0.002$.

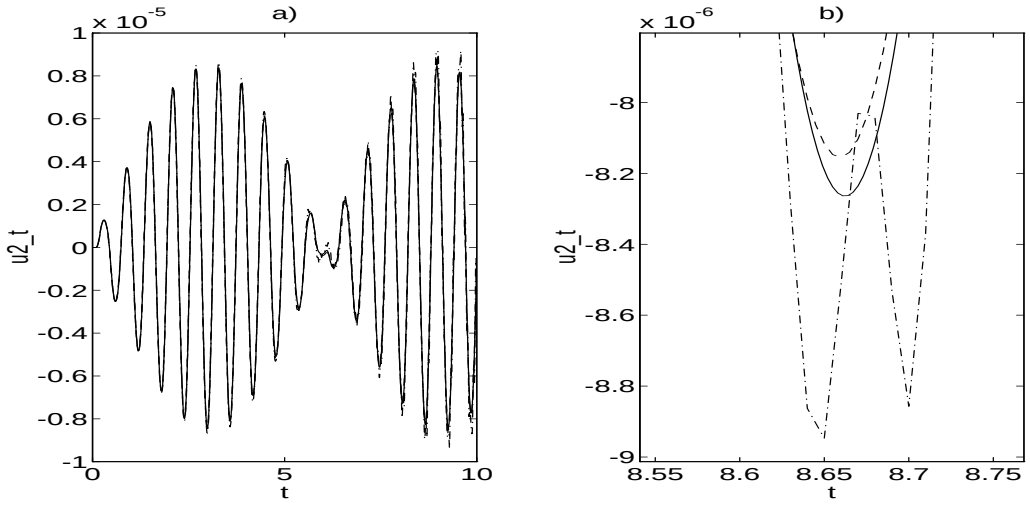

Figure 5: **First test case.** Vertical velocity at $x_2 = -22$ is plotted as a function of time. a) **solid line** – $v_{2,\text{exact}}$, **dashed line** – $v_{2,\text{RK}}$ with $k = 0.005$ and numerical dissipation $\sigma = 5$, **dotted line** – $v_{2,\text{LW}}$ with $k = 0.001$. b) zoom of previous plot.

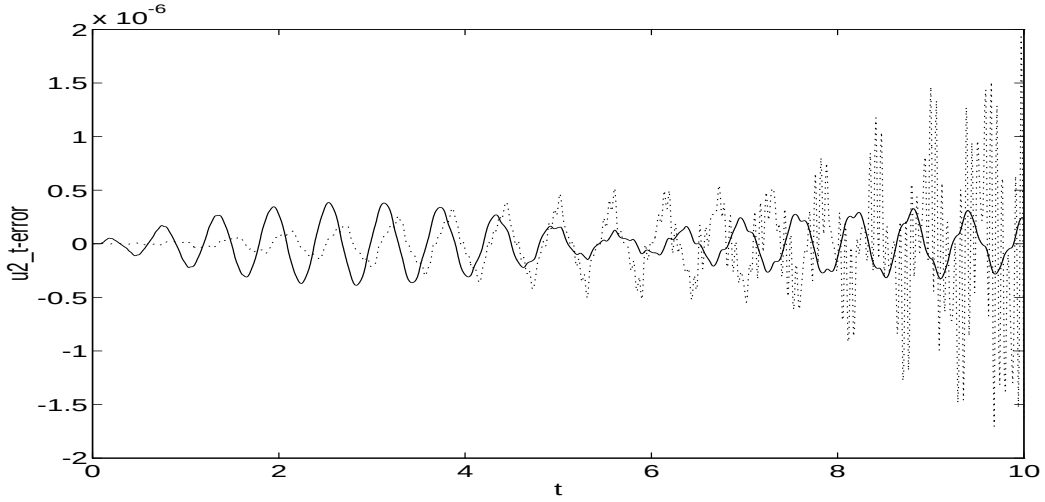

Figure 6: **First test case.** The error of the vertical velocity at $x_2 = -22$ is plotted as a function of time, **solid line** – $v_{2,\text{RK}}$-$v_{2,\text{exact}}$ with $k = 0.005$ and numerical dissipation $\sigma = 5$, **dotted line** – $v_{2,\text{LW}}$-$v_{2,\text{exact}}$ with $k = 0.001$.

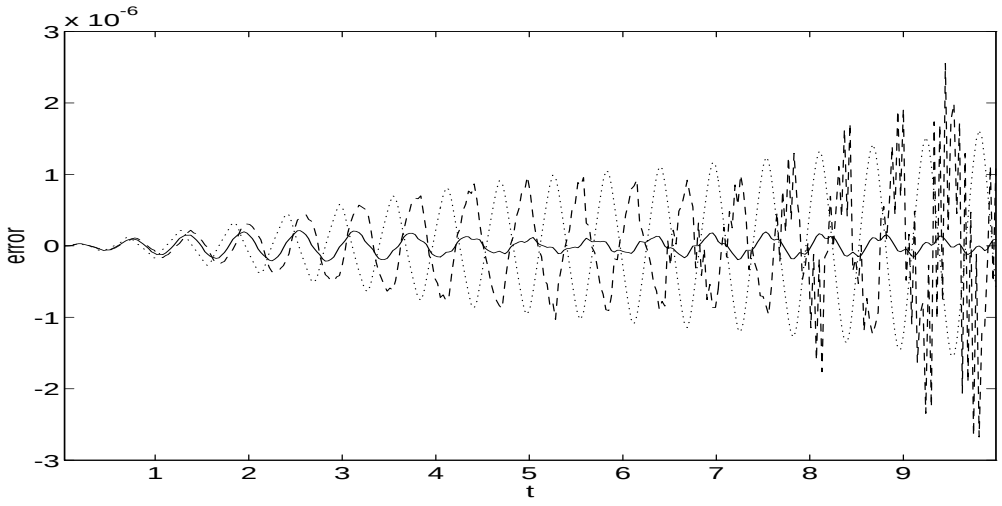

Figure 7: **First test case.** The error of the vertical velocity at $x_2 = -22$ is plotted as a function of time. **solid line** – $v_{2,\mathrm{RK}}$-$v_{2,\mathrm{exact}}$ with $k = 0.003$ and numerical dissipation $\sigma = 5$, **dashed line** – $v_{2,\mathrm{RK}}$-$v_{2,\mathrm{exact}}$ with $k = 0.003$ and numerical dissipation $\sigma = 1$, solution, **dotted line** – $v_{2,\mathrm{RK}}$-$v_{2,\mathrm{exact}}$ with $k = 0.003$ and numerical dissipation $\sigma = 25$.

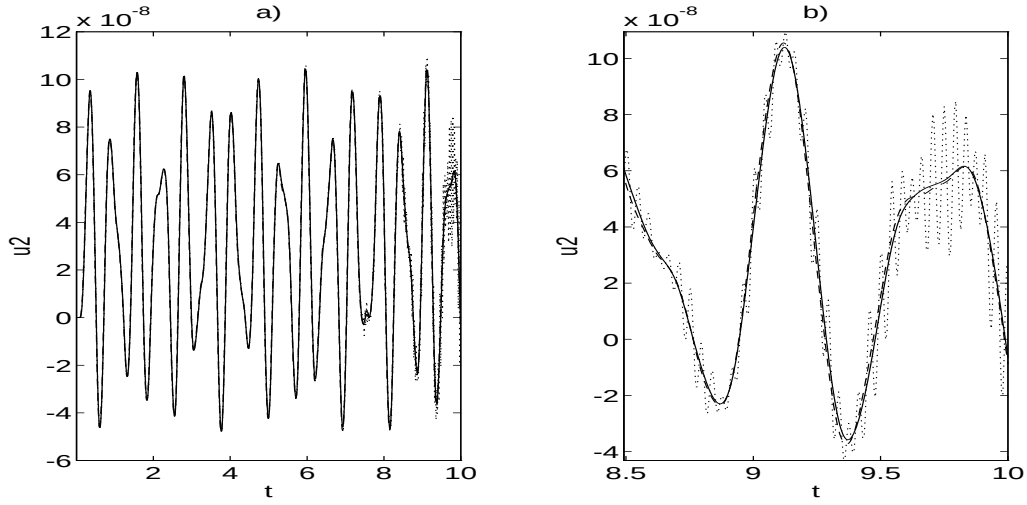

Figure 8: **Second test case.** Vertical displacement at $x_2 = -22$ is plotted as a function of time. a) **solid line** – $u_{2,\mathrm{RK}}$ with $k = 0.005$ and numerical dissipation $\sigma = 5$, **dashed line** – $u_{2,\mathrm{SEC}}$ with $k = 0.001$, **dotted line** – $u_{2,\mathrm{LW}}$ with $k = 0.0005$. b) zoom of previous plot.

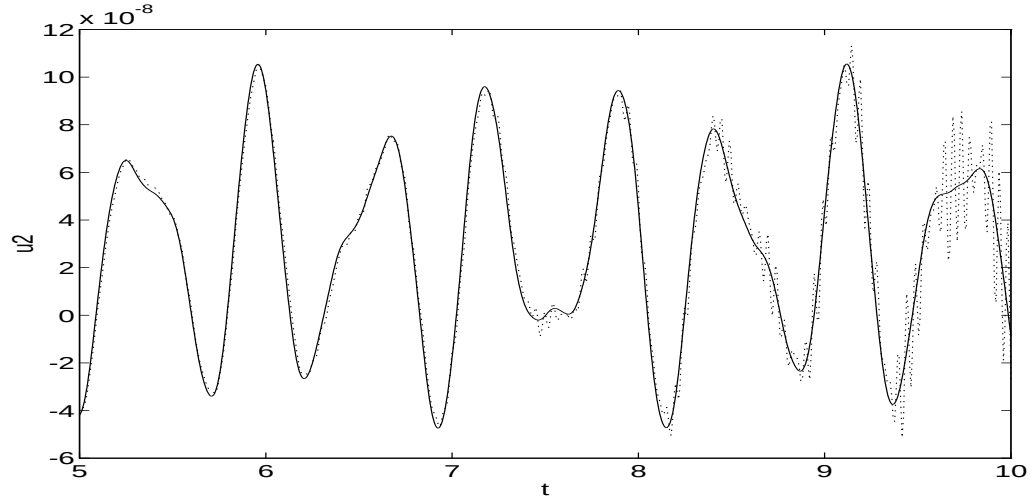

Figure 9: **Second test case.** Vertical velocity at $x_2 = -22$ is plotted as a function of time. a) **solid line** – $v_{2,\mathrm{RK}}$ with $k = 0.005$ and numerical dissipation $\sigma = 5$, **dotted line** – $v_{2,\mathrm{LW}}$ with $k = 0.0005$.

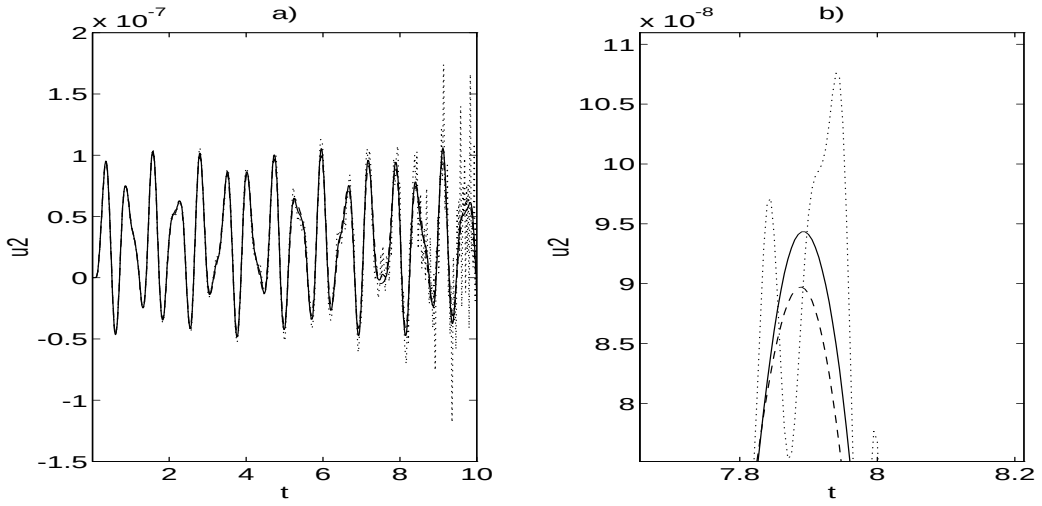

Figure 10: **Second test case.** The vertical velocity at $x_2 = -22$ is plotted as a function of time. a) **solid line** – $v_{2,\mathrm{RK}}$ with $k = 0.005$ and numerical dissipation $\sigma = 5$, **dashed line** – $v_{2,\mathrm{RK}}$ with $k = 0.005$ and numerical dissipation $\sigma = 20$, **dotted line** – $v_{2,\mathrm{RK}}$ with $k = 0.005$ and numerical dissipation $\sigma = 1$. b) zoom of previous plot.

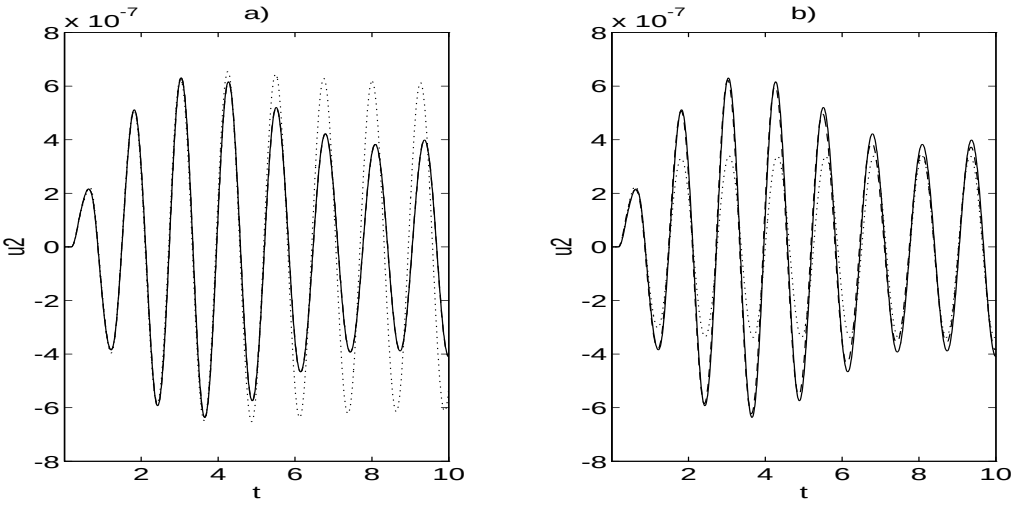

Figure 11: **Third test case.** The vertical displacement plotted as a function of time at $(x_1, x_2) = (9, -22)$. a) solutions from SEC with $k = 0.003$ and material damping $\alpha = 0.05,\ \beta = 0.0005$. **solid line** – $u_{2,SEC}$ with domain Ω_3, **dashed line** – $u_{2,SEC}$ with domain Ω_2, **dotted line** – $u_{2,SEC}$ with domain Ω_1. b) solution from RK with $k = 0.008$ and numerical dissipation $\sigma = 5$. **solid line** – $u_{2,SEC}$ with domain Ω_3, **dashed line** – $u_{2,RK}$ with domain Ω_2, **dotted line** – $u_{2,RK}$ with domain Ω_1.

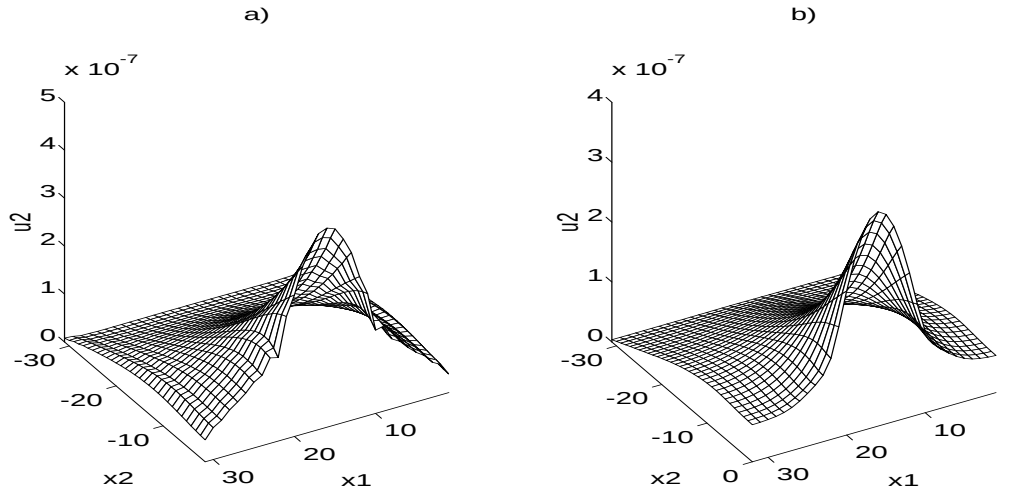

Figure 12: **Third test case.** The vertical displacement at time 0.4s. a) solution from RK with $k = 0.002$ and numerical dissipation $\sigma = 5$, b) solution from SEC with $k = 0.001$ and damping constants $\alpha = 0.1,\ \beta = 0.001$.

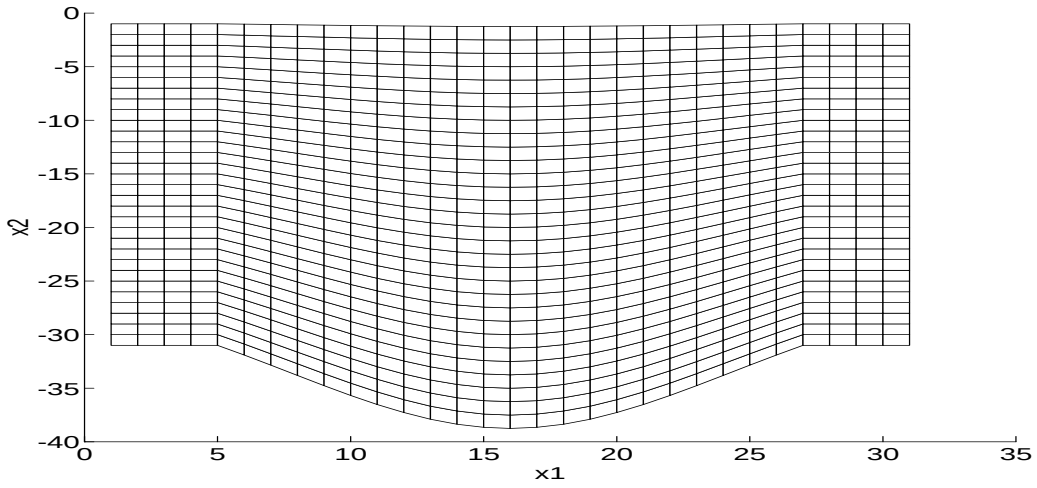

Figure 13: **Fourth test case.** The used grid without boundary points mapped onto the physical domain.

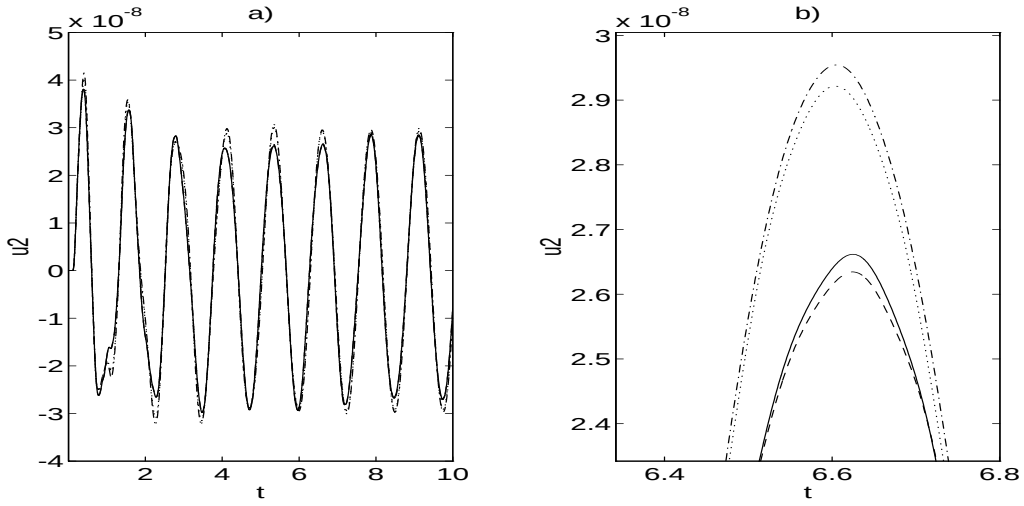

Figure 14: **Fourth test case.** The vertical displacement plotted as a function of time at $(x_1, x_2) = (9, -22)$. Solutions from SEC with $k = 0.001$ and material damping $\alpha = 0.05$, $\beta = 0.0005$. a) **solid line** – $u_{2,SEC}$ with domain Ω_{c3} and $h_1 = h_2 = 1$, **dashed line** – $u_{2,SEC}$ with domain Ω_{c2} and $h_1 = h_2 = 1$, **dash dotted line** – $u_{2,SEC}$ with domain Ω_{c1} and $h_1 = h_2 = 0.5$, **dotted line** – $u_{2,SEC}$ with domain Ω_{c1} and $h_1 = h_2 = 1$. b) zoom of previous plott.

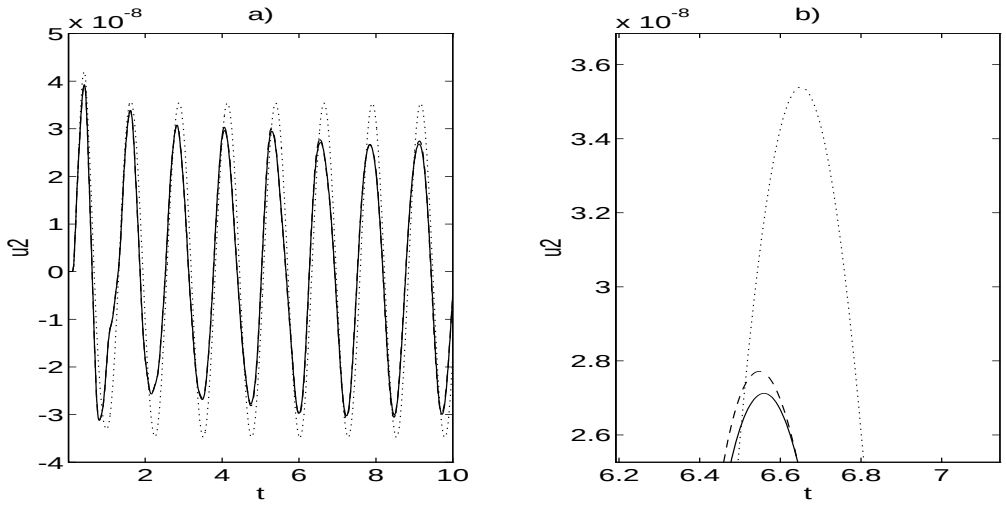

Figure 15: **Fourth test case.** The vertical displacement plotted as a function of time at $(x_1, x_2) = (9, -22)$. Solutions from RK with $k = 0.005$ and numerical dissipation $\sigma = 5$. a) **solid line** – $u_{2,RK}$ with domain Ω_{c3} and $h_1 = h_2 = 1$, **dashed line** – $u_{2,RK}$ with domain Ω_{c2} and $h_1 = h_2 = 1$, **dotted line** – $u_{2,RK}$ with domain Ω_{c1} and $h_1 = h_2 = 1$. b) zoom of previous plott.

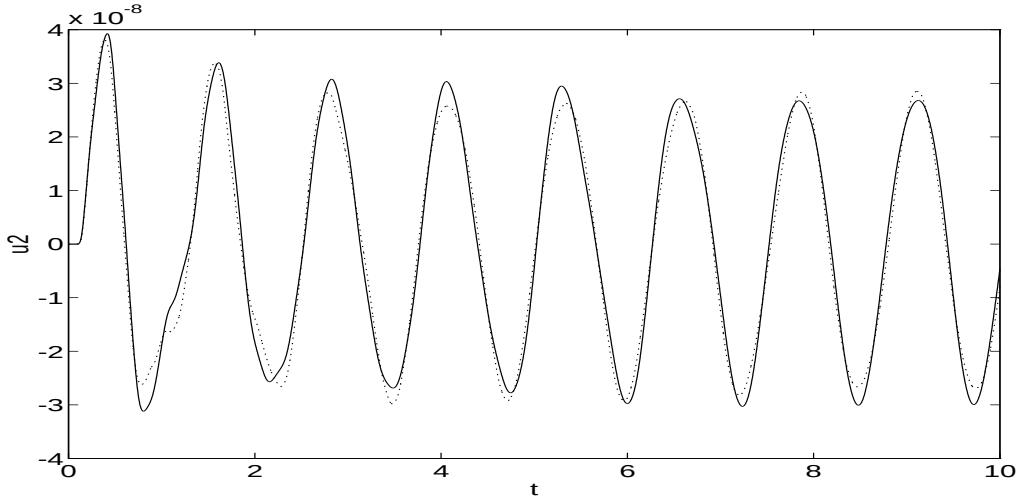

Figure 16: **Fourth test case.** Comparison of the vertical displacements from SEC and RK at $(x_1, x_2) = (9, -22)$. **solid line** – $u_{2,RK}$ with domain Ω_{c3}, $h_1 = h_2 = 1$, $k = 0.005$ and numerical dissipation $\sigma = 5$. **dotted line** – $u_{2,SEC}$ with domain Ω_{c3}, $h_1 = h_2 = 1$, $k = 0.001$ and material damping $\alpha = 0.05$, $\beta = 0.0005$.

3.8 Conclusions

It is possible use a velocity-stress formulation for efficient numerical simulation of two dimensional elastic vibrations. The Lax-Wendroff's method was not computationally competitive with the method of lines based on second order central finite differences in space and time integration by classical fourth order Runge-Kutta. In both cases the accuracy of the discretization of the boundary conditions are of order two which implies global second order accuracy. The timestep limitation for stability in the variable coefficient case agrees well with the theory for the corresponding constant coefficient Cauchy problems. But the accuracy and computational effectiveness of the second order system (displacement formulation) is better than of the first order system (velocity-stress formulation). In particular, the accuracy of the absorbing boundary condition is much better for the second order system. However, it may be easier to use variable steplength in space [ZLS], derive stable higher order methods for the initial-boundary value problem [O] and have discontinuous Lamé parameters for the first order system than for the second order system.

3.9 Acknowledgment

My advisor, Professor Björn Engquist for his guidance and time. Letterstedtska resestipendiefonden and Stiftelsen Lars Hiertas Minne for their financial supports, which made my visit to University of California, Los Angeles, possible.

3.A Analytic solution of an initial-boundary value problem

Consider the initial-boundary value problem (IBVP),

$$\bar{u}_t = \underbrace{\begin{pmatrix} 0 & a_{12} \\ a_{21} & 0 \end{pmatrix}}_{=A} \bar{u}_x, \quad -L < x < 0, \tag{A1a}$$

with initial data

$$\bar{u}(x,0) = 0, \quad -L < x < 0, \tag{A1b}$$

and boundary data

$$\begin{pmatrix} 1 & 0 \\ 0 & 0 \end{pmatrix} \bar{u}(0,t) + \begin{pmatrix} 0 & 0 \\ 0 & 1 \end{pmatrix} \bar{u}(-L,t) = \begin{pmatrix} f(t) \\ 0 \end{pmatrix}, \quad t > 0. \tag{A1c}$$

We shall solve this IBVP with *the method of characteristics* [KL]. Assume that $a_{12}a_{21} > 0$. Then set

$$\bar{v} = T^{-1}\bar{u},$$

where T diagonalize A and $\bar{v}$ are the so-called *characteristic variables*. Here

$$T = \begin{pmatrix} 1 & 1 \\ \sqrt{\frac{a_{21}}{a_{12}}} & -\sqrt{\frac{a_{21}}{a_{12}}} \end{pmatrix},$$

and

$$T^{-1} = \frac{1}{2} \begin{pmatrix} 1 & \sqrt{\frac{a_{12}}{a_{21}}} \\ 1 & -\sqrt{\frac{a_{12}}{a_{21}}} \end{pmatrix},$$

so

$$T^{-1}AT = \begin{pmatrix} \sqrt{a_{12}a_{21}} & 0 \\ 0 & -\sqrt{a_{12}a_{21}} \end{pmatrix} = \begin{pmatrix} \lambda_1 & 0 \\ 0 & \lambda_2 \end{pmatrix} = \Lambda.$$

Write IBVP (A1) in the new variable $\bar{v}$

$$\bar{v} = \Lambda \bar{v}_x, \quad -L < x < 0, \tag{A2a}$$

with initial data

$$\bar{v}(x,0) = 0, \quad -L < x < 0, \tag{A2b}$$

and boundary data

$$\begin{pmatrix} 1 & 0 \\ 0 & 0 \end{pmatrix} T\bar{v}(0,t) + \begin{pmatrix} 0 & 0 \\ 0 & 1 \end{pmatrix} T\bar{v}(-L,t) = \begin{pmatrix} f(t) \\ 0 \end{pmatrix}, \quad t > 0,$$

or

$$\frac{1}{2}\begin{pmatrix} 1 & 1 \\ 0 & 0 \end{pmatrix} \bar{v}(0,t) + \frac{1}{2}\begin{pmatrix} 0 & 0 \\ \sqrt{\frac{a_{21}}{a_{12}}} & -\sqrt{\frac{a_{21}}{a_{12}}} \end{pmatrix} \bar{v}(-L,t) = \begin{pmatrix} f(t) \\ 0 \end{pmatrix}, \quad t > 0. \tag{A2c}$$

The new IBVP has decoupled equations but the boundary data is coupled. Since Λ is a constant diagonal matrix the characteristics are straight lines and thus,

$$v_j(x,t) = v_j(x + \lambda_j t, 0) = 0, \quad -L < x + \lambda_j t < 0.$$

By continuing this process, see figure 17, we can solve the IBVP (A2) exact and then transform $\bar{v}$ back to the original variables $\bar{u}$.

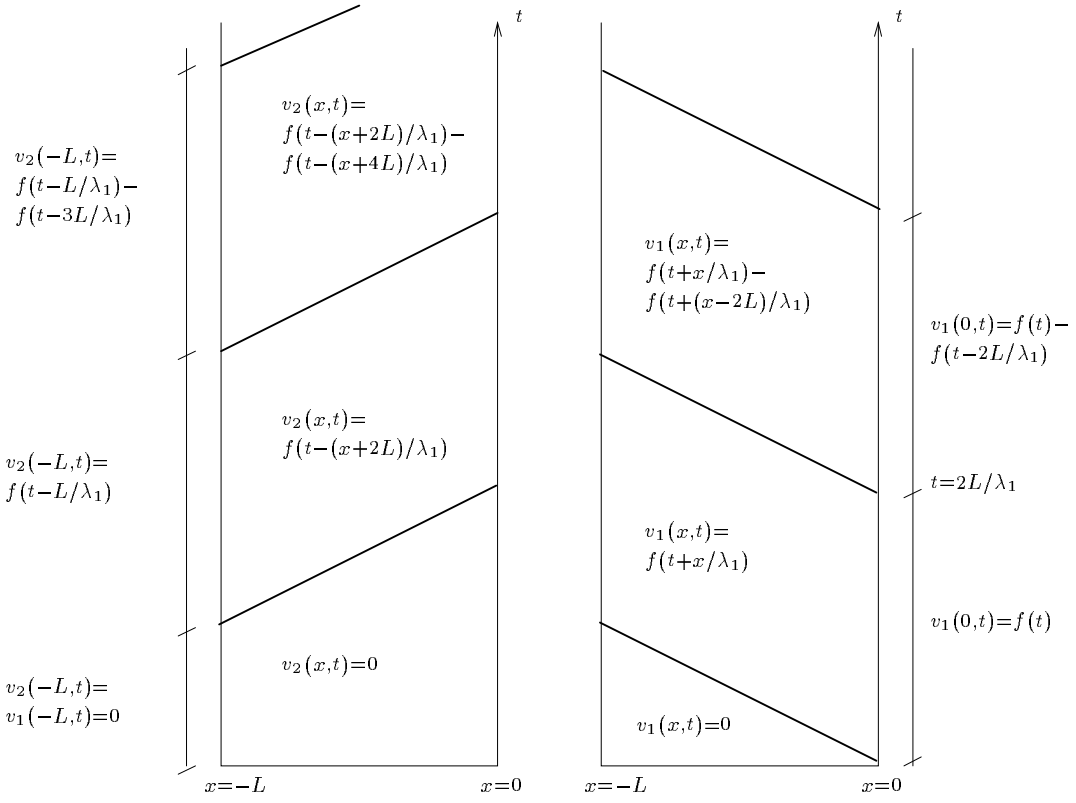

Figure 17: Solution of the IBVP (A1) by the method of characteristics.

References

[A] B. Andreasson. *Deformation Characteristics of Soft High-Plastic Clays under Dynamic Loading Conditions.* PhD Thesis, Chalmers University of Technology, Göteborg, Sweden, 1979.

[B] K. J. Bathe. *Finite Element Procedures in Engineering Analysis.* Prentice-Hall, Inc., 1982

[BD] A. Bedford and D.S. Drumheller. *Introduction to Elastic Wave Propagation.* John Willey & Sons, 1993.

[CE] R. Clayton and B. Engquist. *Absorbing boundary conditions for acoustic and elastic wave equations.* Bulletin of the Seismological Society of America, 67(6):1519–1540, December 1977.

[E] S. Erlingsson. *Dynamic Soil Analysis with an Application to Rock Music Induced Vibrations in Ullevi Stadium.* PhD Thesis, Royal Institute of technology, Stockholm, Sweden, 1993.

[EM] B. Engquist and A. Majda. *Absorbing boundary conditions for numerical simulation of waves.* Math. Comp., 31:629–651, 1977.

[GK] B. Gustafsson and H.-O. Kreiss. *Boundary conditions for Time Dependent Problems with an Artificial Boundary.* J. of Comp. Phys., 30:333–351, 1979.

[GKS] B. Gustafsson, H.-O. Kreiss and A. Sundström. *Stability Theory of Difference Approximations for Mixed Initial Boundary Value Problems. II.* Math. Comp., 26:649–686, 1972.

[J] F. John. *Partial Differential Equations. 4. ed.* Springer-Verlag, 1991.

[K] H.-O. Kreiss. *Über die Differenzapproximation hoher Genauigkeit bei Anfangswertproblemen für partielle Differentialgleichungen.* Numerische Mathematik, 1:186–202, 1959.

[KGO] B. Gustafsson, H.-O. Kreiss and J. Oliger. *Time dependent Problems and Difference Methods.* (to appear) 1994.

[KL] H.-O. Kreiss and J. Lorenz. *Initial-Boundary Value Problems and the Navier-Stokes Equations.* Academic Press, Inc., 1989.

[LW1] P. D. Lax and B. Wendroff. *Systems of conservation laws.* Comm. Pure Appl. Math., 13:217–237, 1960.

[LW2] P. D. Lax and B. Wendroff. *Difference Schemes for Hyperbolic Equations with Higher Order of Accuracy.* Comm. Pure Appl. Math., 17:381–398, 1964.

[R] C. J. Randall. *Absorbing boundary conditions for the elastic wave equation: velocity-stress formulation.* Geophysics, 54:1141–1152, 1989.

[O] P. Olsson. *High-order difference methods and dataparallel implementation.* PhD Thesis, Uppsala University, Uppsala, Sweden, 1992.

[RM] R. D. Richtmeyer and K. W. Morton. *Difference Methods for Initial-Value Problems.* Interscience Publisher, 1967.

[TK] E. Tessmer and D. Kossloff. *3-D elastic modeling with surface topology by a Chebyshev spectral method.* Geophysics, 59:464–473, 1994.

[V] J. Virieux. *P-SV wave propagation in heterogeneous media: Velocity-stress finite difference method.* Geophysics, 51:888–901, 1986.

[ZLS] J. Zahradník, P. O'Leary and J. Sochacki. *Finite-difference schemes for elastic waves based in the integration approach.* Geophysics, 59:928–937, 1994.